

# Modeling mass transport of propylene polymerization on Ziegler–Natta catalyst

Yuan Chen, Xinggao Liu\*

National Laboratory of Industrial Control Technology, Institute of Systems Engineering, Zhejiang University, Hangzhou 310027, China

Received 12 May 2005; received in revised form 12 July 2005; accepted 13 July 2005

Available online 10 August 2005

## Abstract

In the present article, a comprehensive mathematical model for single particle propylene polymerization mainly extended from polymeric multigrain model (PMGM) and multigrain model (MGM) has been developed to describe kinetic behavior, molecular weight distribution, monomer concentration, degree of polymerization and polydispersity index (PDI) for slurry-phase propylene polymerization using heterogeneous Ziegler–Natta catalysts. The modified model gives a more valid mathematical description by accounting for the monomer diffusion phenomena at two levels, namely, taking the effect of monomer diffusion at both the macro- and microparticle levels into account, and the latter is aside from the subject under consideration by PMGM. It has been observed that the present model can predict higher values of polydispersity index (PDI about 6–25) with obtaining some results which are more applicable to the conditions existing in most polymerizations of industrial interest such as the reasonable monomer concentration at the center of particles throughout polymerization process and the effect come nearer to the actual physical process of the initial radius of macro- and microparticles as well when using single-site, non-deactivating catalyst. Further, special attention is also paid in this article to discuss the computational rate, which is the most disadvantage of MGM. It has been shown that the significant computational time saving is also acquired by employing the novel solution methodology.

© 2005 Elsevier Ltd. All rights reserved.

*Keywords:* Modeling; Propylene polymerization; Polydispersity index

## 1. Introduction

Olefin polymerization on Ziegler–Natta catalysts is gaining importance due to widening of the polymer properties window. It is obviously complex and requires to be treated at widely different length scales. According to many open literatures on the engineering aspects of Ziegler–Natta polymerizations of several monomers, and particularly of propylene, one can associate different characteristic lengths and phenomena with three different levels [3]: Macroscale, mesoscale and microscale, respectively. This article concentrates on mesoscale phenomena. For more information on mesoscale models, the diffusional resistances with supported heterogeneous Ziegler–Natta

catalyzed propylene polymerization has been modeled in form of the solid core model (SCM) [17,23], the polymeric flow model (PFM) [8,23,25,27] and later more elaborately as the multigrain model (MGM) [2,7,9,17,26] and polymeric multigrain model (PMGM) [21,22].

SCM does not assume the fragment of catalyst particle and the polymer is considered to grow around a solid catalyst core with all active sites located on its surface. This assumption is obviously in contradiction with experimental observations and model cannot predict broad MWDs for single type of active site only if the concentration of monomer at the surface of the catalyst changes significantly due to the increasing mass diffusion resistance caused by the deposition of the polymer chains around the particle during the course of polymerization. The PFM, first proposed by Schmeal and Street [23] which considering only Fickian diffusion lead to monomer transfer assumes growing polymer chains and catalyst fragments form a continuum. If the polymerization is diffusion controlled, namely only at Thiele modulus values greater than  $\sqrt{10}$ , the radial profiles of monomer in the particle may cause significant MWD broadening. This class

\* Corresponding author. Tel.: +86 571 87951970 404; fax: +86 571 87951068.

E-mail address: [liuxg@iipc.zju.edu.cn](mailto:liuxg@iipc.zju.edu.cn) (X. Liu).

**Nomenclature**

$C^*$	catalyst active site concentration ( $\text{mol site m}^{-3}$ )	$P_0$	concentration of empty sites ( $\text{mol m}^{-3}$ catalyst)
$D_{\text{ef},i}$	effective macroparticle diffusion coefficient, at $i$ th grid point ( $\text{m}^2 \text{s}^{-1}$ )	$P_n$	concentration of sites with a growing chain of $n$ monomer units attached ( $\text{mol m}^{-3}$ catalyst)
$D_1$	monomer diffusivity in purely polymer ( $\text{m}^2 \text{s}^{-1}$ )	$\bar{Q}$	polydispersity index
$DP_{\text{av}}$	degree of polymerization in the macroparticle	$\bar{Q}$	cumulative polydispersity index
$D_s$	effective microparticle diffusion coefficient	$r$	radial position at the macroparticle level (m)
$k_p$	propagation rate constant ( $\text{m}^3 \text{mol}^{-1} \text{s}^{-1}$ )	$r_s$	radial position at the microparticle level (m)
$k_{\text{tr}}$	chain transfer rate constant, for $\text{H}_2$ ( $\text{m}^{3/2} \text{mol}^{1/2} \text{s}^{-1}$ )	$R_{\text{overall}}$	time-dependent reaction rate ( $\text{kg kg-cat}^{-1} \text{h}^{-1}$ )
$k_1$	liquid film mass transfer coefficient ( $\text{m}^2 \text{s}^{-1}$ )	$R_c$	radius of catalyst subparticles (m)
$\text{H}_2$	concentration of $\text{H}_2$ in the bulk	$R_{N+2}$	macroparticle radius (m)
$M_i$	monomer concentration in the macroparticles, at the $i$ th grid point ( $\text{mol m}^{-3}$ )	$R_0$	initial particle radius (m)
$M_b$	bulk monomer concentration ( $\text{mol m}^{-3}$ )	$R_{h,i}$	the radius of $i$ th hypothetical shells
$M_{c,i}$	modified monomer concentration at the catalyst surface in the microparticle, at the $i$ th hypothesis shell ( $\text{mol m}^{-3}$ )	$R_{s,i}$	the radius of microparticle at $i$ th hypothetical shell
$M_n$	number average molecular weight	$R_{\text{pv},i}$	rate of reaction per unit volume at $i$ th grid point ( $\text{mol (m}^3 \text{h)}^{-1}$ )
$M_{n,k}$	number average molecular weight in the $k$ th shell	$R_g$	universal gas constant ( $\text{Pa m}^3 \text{mol}^{-1} \text{K}^{-1}$ )
$\bar{M}_n$	number average molecular weight in the macroparticle	$T$	time (h)
$M_w$	weight average molecular weight	<i>Greek letters</i>	
$M_{w,k}$	weight average molecular weight in the $k$ th shell	$\alpha$	Thiele modulus of propagation
$\bar{M}_w$	weight average molecular weight in the macroparticle	$\beta_i$	indicator of the monomer convection contribution
MW	molecular weight of monomer ( $\text{g mol}^{-1}$ )	$\varepsilon$	porosity
$N$	initial number of shells	$\rho_c$	density of catalyst, ( $\text{g m}^{-3}$ )
$N_i$	number of catalyst subparticle in $i$ th shell monomer units attached ( $\text{mol m}^{-3}$ catalyst)	$\rho_p$	density of polymer ( $\text{g m}^{-3}$ )
		$\varpi_k$	mass fraction of polymer in $k$ th shell
		$\lambda$	moment of live polymer ( $P_n$ ) MWD
		$\Lambda$	moment of dead polymer ( $M_n$ ) MWD

of models is a significant improvement over earlier models even though it is not consistent with the large number of experimental values as it does not explicitly consider the fragmentation of the catalyst particle and the values of the parameters used by PFM to generate results are not physically meaningful. MGM more directly takes into account the heterogeneous nature of the growing polymer particle, particularly since it can incorporate catalyst fragmentation, diffusional resistance, as well as active site heterogeneity, the three most important physico-chemical effects, so it is probably the most comprehensive of all the models. The major disadvantage of this model is that the computational times required to obtain the PDIs are extremely high. This makes this model inconvenient for use in more interesting engineering studies like the simulation of industrial reactors, optimization, control etc. For this reason, studies on PMGM by Sarkar et al. leading to the development of more diffusion negligible at the microparticle level, they use a formulation similar to that of Laurence and Chiovetta [12] using specified size and porosity data. The most advantage of this model is that its

solution methodology makes the computational rate improve significantly, especially using clubbed shell computational algorithm (CSA) [22]. Unfortunately, some results from PMGM are not very applicable to the conditions existing in most polymerization of industrial interest, such as the monomer concentration at the centre of the particles drops very quickly to nearly zero, and remains there for over 2 h of polymerization [16] as well as the great effect of the number of microparticles while PMGM think it does not lead to much change in the result which differs from the Nagel's research [17] when varying initial radius of microparticle ( $R_c$ ) with radius of macroparticles ( $R_0$ ) constant.

The purpose of this study is to develop an efficient model, which combines the polymer property, particle morphology and computational time perfectly. In this manuscript, a modified polymeric multigrain model, therefore, has been obtained in our work based upon the relative merits of MGM and PMGM mentioned above. The results about the effect of several important physical parameters on PDI or some relevant outcome in the area of intraintricle mass transfer for propylene polymerization with Ziegler-Natta

catalysts is figured out simultaneously both for industrial and academic applications. Additionally, the computational rate, which is another significant performance indicator of model is also discussed and compared.

### 2. Model description

In the present study, a modified polymeric multigrain model has been developed based on the experimental observation [1,15] that the catalyst is present as small fragments in a polymer continuum. Kakugo’s experiment advanced that all the radius of catalyst subparticle remains same and unchanged after experiencing the instantaneous fragmentation during the process of polymerization. The pores amount the microparticles through which monomer diffuse into the surface of catalyst subparticle and the catalyst subparticles move radially outwards in time. Limiting the consideration now to homopolymerization, spherical catalyst particle, only a single type of active site, heat transfer negligible, [2,6,9,14,27] and retain the assumption of instantaneous fragmentation which are also employed by SCM, PFM, MGM and PMGM to maintain simplicity although the fragmentation process during the polymerization has been modeled [4,5,13,24].

The following well-known diffusion-reaction differential equations are obtained for the concentration,  $M$ , of the

monomer at any radial position,  $r$ , and time,  $t$ , in a single spherical macroparticle:

$$\frac{\partial M}{\partial t} = \frac{D}{r^2} \frac{\partial}{\partial r} \left( r^2 \frac{\partial M}{\partial r} \right) - R_{pv} \tag{1a}$$

$$\frac{\partial M}{\partial r}(r = 0, t) = 0 \tag{1b}$$

$$D_{ef} \frac{\partial M}{\partial r}(r = R_p, t) = k_1(M_b - M) \tag{1c}$$

$$M(r, t = 0) = M_0 = 0 \tag{1d}$$

where  $R_{pv}$  is the volumetric rate of polymerization in the macroparticle,  $D_{ef}$  is the effective diffusivity of monomer in the macroparticle,  $k_1$  is the mass transfer coefficient in the external film,  $M_b$  is the bulk monomer concentration in the reactor.  $M$  and  $M_0$  are the evolving and initial monomer concentrations in the macroparticle, respectively.  $R_p$  is the radius of macroparticle in this model, since the catalyst fragments are assumed to be in a continuum of polymer also employed by Sarkar [21] in PMGM, there is no macroparticle porosity term in Eq. (1), in contrast to that in the multigrain model MGM [6].

The radial profile of monomer concentration in the microparticle is the same as that for the solid core model:

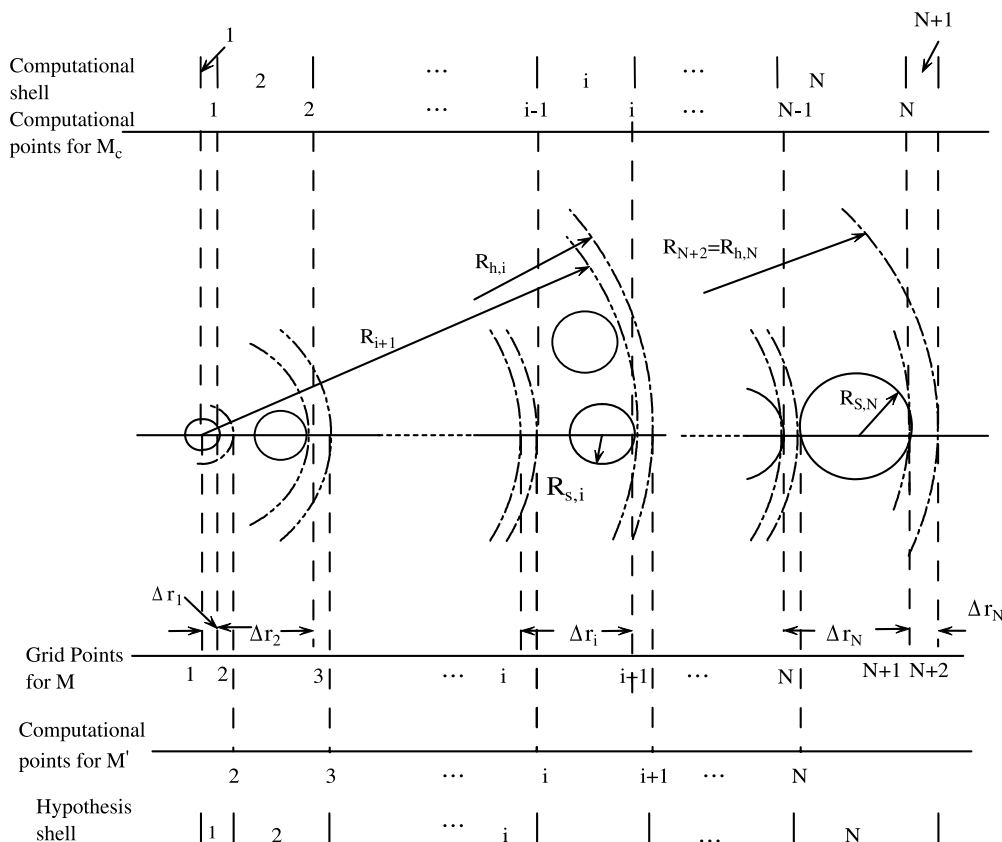


Fig. 1. Catalyst subparticles distribution at time  $t$  in the modified polymeric multigrain model.

$$\frac{\partial M_c}{\partial t} = \frac{1}{r^2} \frac{\partial}{\partial r} \left( D_s r^2 \frac{\partial M_c}{\partial r} \right) \quad (2a)$$

$$4\pi R_c^2 D_s \frac{\partial M_c}{\partial r} (r = R_c, t) = \frac{4}{3} \pi R_c^3 R_{pc} \quad (2b)$$

$$M_c(r = R_s, t) = M^* = \eta^* M \leq M \quad (2c)$$

$$M_c(r, t = 0) = M_{c0} \quad (2d)$$

where  $D_s$  is the effective diffusivity of monomer in the microparticle,  $M^*$  is the equilibrium concentration of monomer in the interface between micro- and macroparticles,  $M_c$  is the monomer concentration in the microparticle,  $R_{pc}$  is the rate of polymerization on the surface of the catalyst fragments, and  $R_s$  is the radius of the microparticle. And boundary condition (2b) allows for the possibility of sorption equilibrium at the surface of the microparticles.

The rate of polymerization on the microparticles is generally given by

$$R_{pc} = k_p(t) C^*(t) M_{SA} \quad (3)$$

where  $M_{SA}$  is the concentration of monomer on the active site and  $C^*(t)$  is the time-dependent concentration of active sites on the surface of the microparticle.

Using the quasi steady state approximation (QSSA) presented in Hutchinson et al. [9],  $M_c$  is easily obtained as

$$M_c = \frac{\eta^* M}{1 + \frac{R_c^2}{3D_s} \left(1 - \frac{R_c}{R_s}\right) k_p C^*} \quad (4)$$

where  $M_c$  is the monomer concentration at the catalyst surface in the microparticle.  $\eta^*$  represents the corresponding equilibrium constant for monomer absorption in the microparticle. We should pay special attention on this point which is ignored by PMGM and this is one of the contributions of this work.

The number of the small particles in any shell,  $N_i$ , are assumed to be unchanged during polymerization progresses and all the catalyst subparticle radii for each microparticle in the  $i$ th shell at a given macroparticle radius are assumed to be all the same size [7,10]. Then Eq. (1) is written in finite difference form to give a set of ordinary differential equations (ODEs) for  $M_i$ , the monomer concentration at each of the  $N+2$  different computational grid points shown in the Fig. 1 and these ODEs are listed as follows:

$$\frac{\partial M_1}{\partial t} = D_{ef,1} \frac{M_2 - M_1}{\Delta r_1^2} - R_{pv,1} \quad (5a)$$

$$\begin{aligned} \frac{\partial M_i}{\partial t} = & D_{ef,i} \left[ M_{i+1} \left( \frac{1}{\Delta r_i R_i} + \frac{1}{\Delta r_i^2} \right) - M_i \left( \frac{1}{\Delta r_i^2} + \frac{1}{\Delta r_{i-1} \Delta r_i} \right) \right. \\ & \left. + M_{i-1} \left( \frac{1}{\Delta r_{i-1} \Delta r_i} - \frac{1}{\Delta r_i R_i} \right) \right] - R_{pv,i}; \end{aligned}$$

$$i = 2, 3, \dots, N + 1$$

(5b)

$$\begin{aligned} \frac{\partial M_{N+2}}{\partial t} = & -M_{N+2} \left[ \frac{k_1}{\Delta r_{N+1}} + \frac{D_{ef,N+2}}{(\Delta r_{N+1})^2} + \frac{2k_1}{R_{N+2}} \right] \\ & + M_{N+1} \left[ \frac{2D_{ef,N+2}}{(\Delta r_{N+1})^2} \right] \\ & + M_b \left( \frac{k_1}{\Delta r_{N+1}} + \frac{2k_1}{R_{N+2}} \right) - R_{pv,N+2} \end{aligned} \quad (5c)$$

here  $R_i$ ,  $\Delta r_i$ ,  $D_{ef,i}$ ,  $R_{pv,i}$  can be computed through the ‘hypothetical’ shell we defined (as in Fig. 1(a)).

According to Fig. 1, the number of subparticles in  $i$ th shell at time  $t=0$ ,  $N_i$ , is calculated using the porosity  $\varepsilon$  which has been taken to be a constant, as in the early MGM [7] just as  $N_i$  in the polymerization process, associated with close-packed sphere:

$$N_1 = 1 \quad (6a)$$

$$N_i = 24(1 - \varepsilon)(i - 1)^2; \quad i = 2, 3, \dots, N \quad (6b)$$

The total volume of polymer,  $V_i$ , and the volume of microparticle at  $i$ th shell,  $V_{s,i}$ , all produced by catalyst particles are given by:

$$\frac{dV_i}{dt} = \frac{0.001 k_p C^* M_{c,i} (N_i \frac{4\pi}{3} R_c^3) (MW)}{\rho_p} \quad (7)$$

$$\frac{dV_{s,i}}{dt} = \frac{0.001 k_p C^* M_{c,i} (\frac{4\pi}{3} R_c^3) (MW)}{\rho_p} \quad i = 1, 2, \dots, N \quad (8)$$

with  $V_i(t=0)$  and  $V_{s,i}(t=0)$  being the initial total volume and volume of every polymer microparticle of  $i$ th volume, respectively.

$$V_i(t=0) = \frac{N_i (\frac{4\pi}{3} R_c^3)}{(1 - \varepsilon)} \quad i = 1, 2, \dots, N \quad (9)$$

$$V_{s,i}(t=0) = \frac{4\pi}{3} R_c^3 \quad (10)$$

and the  $M_{c,i}$  which is modified monomer concentration value of catalyst surface in microparticle at the  $i$ th hypothesis shell,  $R_{h,i}$ , computed by Eq. (4), the detailed form expressed in what follows:

$$M_{c,i} = \frac{\eta^* M'_i}{1 + \frac{R_c^2}{3D_s} \left(1 - \frac{R_c}{R_{s,i}}\right) k_p C^*}$$

$$= \frac{\eta^* M_{i+1}}{1 + \frac{R_c^2}{3D_s} \left(1 - \frac{R_c}{R_{s,i}}\right) k_p C^*} \quad (11)$$

It is obvious that  $M_{i+1}$  is equal to  $M'_i$  for  $i=2,3,\dots,N+1$ , due to they belong to the same computational shell as shown in Fig. 1. This point is amended to perfect PMGM by taking the factor of diffusion at the microparticle level under advisement. The detailed form of Eq. (4) is originated from this reason.

The hypothetical shells,  $R_{h,i}$ , can be defined at any time whose physical meaning of a already refer to when describe  $M_c$  by:

$$R_{h,i} = \left( \frac{3}{4\pi} \sum_{j=1}^i V_j \right)^{1/3}; \quad i = 1, 2, \dots, N \quad (12)$$

where  $R_{h,0}=0$  and the radius of microparticle at  $i$ th shell being:

$$R_{s,i} = \left( \frac{3}{4\pi} V_{s,i} \right)^{1/3} \quad (13)$$

The catalyst particles are assumed to be placed at the mid-points of each hypothetical shell:

$$R_{1,i} = R_{h,i-1} + \frac{1}{2}(R_{h,i} - R_{h,i-1}) \quad i = 2, 3, \dots, N \quad (14)$$

Then the computational grid points are related to  $R_{1,i}$  by:

$$R_1 = 0 \quad (15a)$$

$$R_2 = R_c \quad (15b)$$

$$R_{i+1} = R_{1,i} + R_{s,i}; \quad i = 2, 3, \dots, N \quad (15c)$$

Here  $R_{N+2}=R_{h,N}$ . Thus the values of  $\Delta r_i$  to be used in the equations of Table 1 are given by:

$$\Delta r_i = R_{i+1} - R_i \quad i = 1, 2, \dots, N + 1 \quad (16)$$

To account for the resistance due to the presence of the solid catalyst fragments after finishing all previous work, an effective diffusivity is introduced to this equation. Most models have tried to related the effective diffusivity,  $D_{\text{eff}}$ , to the value of the diffusivity of the component in question in the bulk phase of the reactor,  $D_1$ . Using the expression

commonly used for heterogeneous catalysts:

$$D_{\text{eff}} = D_1 \frac{\varepsilon}{\tau} \quad (17)$$

where  $\varepsilon$  and  $\tau$  are the porosity and tortuosity of the macroparticle, respectively. Note that due to the macroparticle fragmentation and growth, it is very likely that both  $\varepsilon$  and  $\tau$  are functions of time as well as radial position. Sarkar and Gupta make the diffusivity be corrected by a factor proportional to the amount of polymer in the particles, i.e. the term  $\varepsilon/\tau$  of above-mentioned equation for a correction factor equal to the area-fraction of polymer (assumed to be the same as its volume fraction) in the macroparticle at any radial location. Thus, as the particle fills up with polymer, the effective diffusivity decrease as follows:

$$D_{\text{ef},1} = D_{\text{ef},N+2} = D_1 \quad (18a)$$

$$D_{\text{ef},2} = D_1 N_1 \frac{R_c^3}{R_{h,1}^3} \quad (18b)$$

$$D_{\text{ef},i+1} = D_1 \frac{(V_{cs,i} - V_{cc,i})}{V_{cs,i}} = D_1 \frac{R_{h,i}^3 - R_{h,i-1}^3 - N_i R_c^3}{R_{h,i}^3 - R_{h,i-1}^3} \quad (18c)$$

where  $D_1$  is the diffusion of monomer through pure polymer and  $D_{\text{ef},1}=D_{\text{ef},N+2}=D_1$ .  $V_{cs,i}$  and  $V_{cc,i}$  being the volume of the  $i$ th hypothesis shell and the volume of catalyst in shell  $i$ , respectively. So the effective diffusion coefficient here is considered to be change any time during particle growth in opposition to [6].

Then as the net rate of consumption of monomer per unit macroscopic volume at any radial location,  $R_{\text{pv}}$ , at the mean time, also can be figured out by:

$$R_{\text{pv},1} = R_{\text{pv},N+2} = 0 \quad (19a)$$

$$R_{\text{pv},2} = \frac{k_p C^* M_{c,1} N_1 R_c^3}{R_{h,1}^3} \quad (19b)$$

$$R_{\text{pv},i} = \frac{k_p C^* M_{c,i-1} N_{i-1} R_c^3}{R_{h,i}^3 - R_{h,i-1}^3} \quad (19c)$$

where  $R_{\text{pv},1}=R_{\text{pv},N+2}=0$ . So the corresponding overall time-dependent reaction rate can be calculated:

$$R_{\text{overall}} = \frac{0.001(\text{MW})k_p C^* \sum_{i=1}^N (N_i M_{c,i})}{\rho_c \sum_{i=1}^N N_i} \quad (20)$$

In heterogeneously catalyzed propylene polymerization, the monomer concentration at catalyst active sites surface should be known to calculate the overall time-dependent particle polymerization rate, given by Eq. (20). In solid-catalyzed polymerizations, the polymer grows at the active

Table 1

Simplified kinetic mechanism of Ziegler–Natta catalyzed propylene polymerization

Description	Reaction
Initiation	$P_0 + M_c \xrightarrow{k_p} P_1$
Propagation	$P_n + M_c \xrightarrow{k_p} P_{n+1}$
Termination	$P_n + 1/2H_2 \xrightarrow{k_t} D_n + P_1$

sites of the catalyst until chain transfer occurs, or the site is deactivated.

Thus, there is present ‘live’ polymer, which is still attached to an active site, and ‘dead’ polymer, which has at its end a group from a chain transfer or deactivating agent. The moment of the live and dead polymer can be calculated, using the method also outlined by Floyd. Table 1 gives the simplified kinetic mechanism of Ziegler–Natta catalyzed propylene polymerization. Application of the method for solid-catalyzed olefin polymerization is described below. From Table 1,  $P_0$  represents the unreacted active catalyst sites, while  $P_n$  and  $D_n$  are the concentration of live and dead polymer of chain length  $n$ , respectively. Both the rate constants for initiation, propagation are  $k_p$  and  $k_{tr}$ , for termination by chain transfer to hydrogen. In this work, only the chain transfer with hydrogen is considered to avoid adding more complexity of the model due to its predominates [20]. Detailed description on material balance, moment equation and the computational method of PDI has already been particularly noted by some open literatures [7,8].

### 3. Results and discussion

All of the results presented below in this paper are used to explain the broad MWD obtained during polymerization with Ziegler–Natta catalysts and study the advantage of the modified PMGM which also amounts to a significant computational simplification by computing the sets of ordinary differential equations demonstrated above in detail. We also speculate the effects of various parameters such as catalyst propagation rate constant  $k_p$ , the radius of catalyst subparticles ( $R_c$ ), initial radius of macroparticle at  $t=0$  ( $R_0$ ), catalyst active site concentration ( $C^*$ ) on time-dependent polymerization rate ( $R_{overall}$ ) and cumulative polydispersity index ( $Q_{av}$ ) and so on. These simulations included the effects of external mass transfer by diffusion, assuming  $k_p$  and  $k_{tr}$  are independent of the type of active site, taking no

account of catalyst decay which is also employed by Sarkar [21].

A PMGM program is developed from Sarkar [21,22] simultaneously as a basis of comparison and a set of reference values have been selected for the parameters listed in Table 2 as also employed by Sarkar et al. for slurry-phase polymerization of propylene in order to make it convenient to have a comparison with PMGM [19,30]. A parametric sensitivity study is conducted by varying some of the parameters of our present model one by one while remaining all other values invariable. Analyses are then carried out in connection with some unreasonable results, which are not applicable to the conditions existing in most polymerizations of industrial interest in PMGM as below.

#### 3.1. Comparison on $Q_{av}$ and $M$ of PMGM and modified PMGM

Fig. 2 shows the comparison of cumulative polydispersity index ( $Q_{av}$ ) and the distribution of monomer concentration in the macroparticle between modified PMGM and PMGM for the reference conditions in Table 2. In theory, the diffusion resistance abandoned by PMGM obviously exists and should be put up in the mesoscale model [28]. The modified PMGM, however, revised it and can predict higher values of polydispersity index from 6 to 25 compared with that of PMGM (from 4 to 15) due to the steeper modified monomer concentration profile in the catalyst macroparticles which is more reasonable as talking in physics meaning.

The monomer concentration at the macroparticle level of PMGM as showed in Fig. 2(b) is not applicable to the conditions existing in most polymerization of industrial interest since the monomer concentration at the centre of the particles drop very quickly to nearly zero and remains there for over 2 h of polymerization [16]. The proposed model modified it, which is displayed in Fig. 2(b) with dash-dot line and the monomer concentration at the centre of the particle is about  $1800 \text{ mol m}^{-3}$  after 1.5 h polymerization reaction which comes closer to the industrial practice.

#### 3.2. Effect of the radius of microparticle

Results for the modified PMGM are also generated under the conditions of changing the radius of microparticle ( $R_c$ ) while remaining the initial particle radius ( $R_0$ ) constant. Nagel et al. [17] notes that it has a strong effect on polydispersity when varying the number of microparticle with other conditions constant. PMGM indicates, however, that there is not much change to the results under such circumstance. This result does not correspond to the actual physical process obviously. It is revised by this modified PMGM and can be observed from Fig. 3 that  $Q_{av}$  of the polymer decreases while  $DP_{av}$  increases when  $R_0$  is lowered from 14.2 to 7.1  $\mu\text{m}$  in the condition that all other values being equal. The reason why  $DP_{av}$  are higher for

Table 2  
Reference values of parameters for simulation of slurry polymerization of propylene

Parameter	Value	Unit
$D_l$	$1 \times 10^{-11}$	$\text{m}^2 \text{s}^{-1}$
$D_s$	$1 \times 10^{-12}$	$\text{m}^2 \text{s}^{-1}$
$M_b$	$4 \times 10^3$	$\text{mol m}^{-3}$
$R_c$	$2 \times 10^{-7}$	m
$C^*$	1	$\text{mol site m}^{-3} \text{cat}^{-1}$
$k_p$	0.5	$\text{m}^3 \text{mol site s}^{-1}$
$k_{tr}$	0.186	$\text{m}^{3/2} \text{mol}^{-1/2} \text{s}^{-1}$
$H_2$	1	$\text{mol m}^{-3}$
$k_1$	$1 \times 10^{-3}$	$\text{m s}^{-1}$
$\rho_p$	900	$\text{kg m}^{-3}$
$\rho_c$	2260	$\text{kg m}^{-3}$
$R_0$	$1.42 \times 10^{-5}$	m

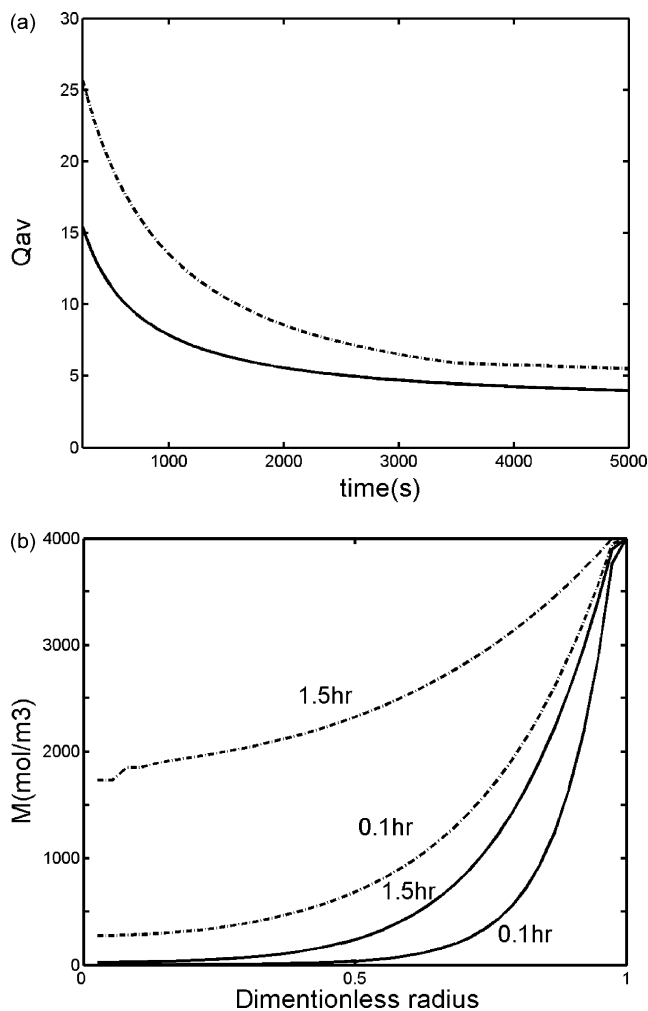


Fig. 2. Comparison of cumulative polydispersity index ( $Q_{av}$ ) and monomer concentration profile between modified PMGM (dash-dot line) and PMGM (solid line).

lower values of  $R_0$  is because of lower diffusional resistances encountered in smaller catalyst particles so to make the difference of monomer concentration between inside and outside of the particle diminish. And we also found that  $DP_{av}$  is very sensitive to the parameter of  $R_c$  when retaining  $C^*$  constant, namely,  $C^*$  have no connection with the total surface area of the microparticle. Similarity as Fig. 3 showed that  $DP_{av}$  and  $Q_{av}$  go in an opposite direction, the former increases while the latter decreases when varying  $R_c$  from 0.3 to 0.1  $\mu\text{m}$  at the same value of  $R_0$ . So with single site catalysts, both larger initial catalyst particles and larger subparticles can give rise to high PDIs.

### 3.3. Effect of $k_p$ and $C_x$

This fraction turns the attention to the study of the effects of parameter variation for the modified PMGM. The effect of varying the three different catalyst activities, or, equivalently, the catalyst active site concentration,  $C^*$  are

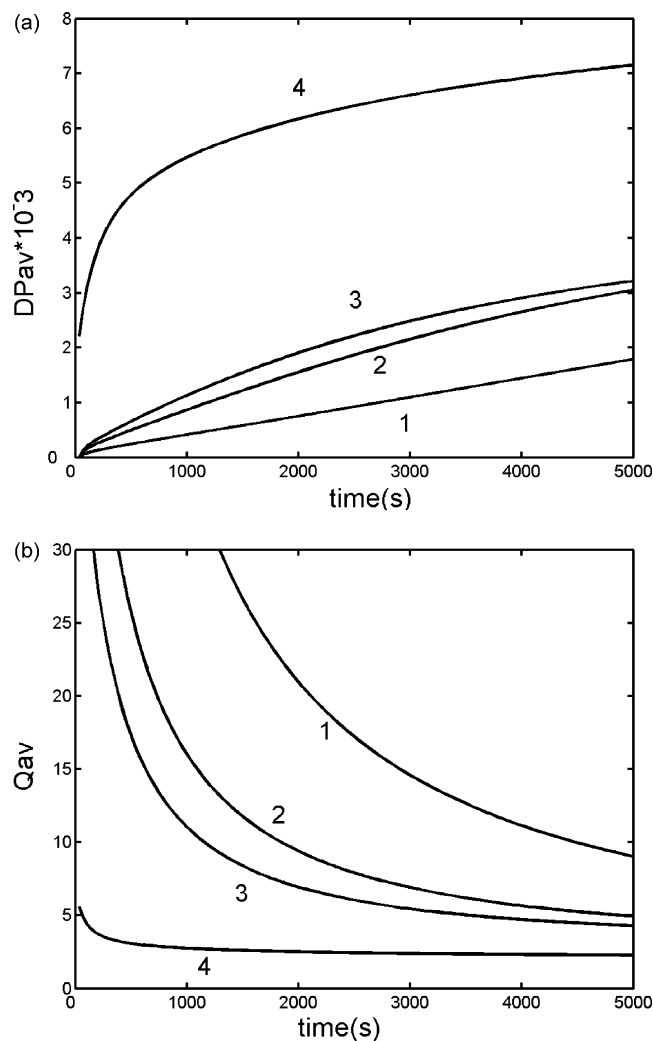


Fig. 3. Effect of change in  $R_c$  while maintaining  $R_0$  unchanged on (a) degree of polymerization ( $DP_{av}$ ), (b) cumulative polydispersity index ( $Q_{av}$ ). (1)  $R_c=0.3 \mu\text{m}$ ,  $R_0=14.2 \mu\text{m}$ ; (2)  $R_c=0.2 \mu\text{m}$ ,  $R_0=14.2 \mu\text{m}$ ; (3)  $R_c=0.1 \mu\text{m}$ ,  $R_0=14.2 \mu\text{m}$ ; (4)  $R_c=0.1 \mu\text{m}$ ,  $R_0=7.1 \mu\text{m}$ .

first studied. The value of the catalyst activity for  $k_p=0.25$ , 0.5, 1  $\text{m}^3 \text{mol s}^{-1}$ , and  $C^*=0.5$  and  $C^*=1 \text{mol site m}^{-3}$ , respectively. Fig. 4 shows that both monomer concentration gradient in the macroparticle and cumulative polydispersity index are higher by increasing the value of  $k_p$ . And it is observed that  $Q_{av}$  is very sensitive to this parameter when  $k_p$  increase up to 0.5. The reason why there are higher  $Q_{av}$  and steeper  $M_c$  gradient (lower  $DP_{av}$ ) for the higher  $k_p$  is because the effect on  $Q_{av}$  produced by monomer diffusion is weakened since the influence of  $k_p$  predominates with its rise. A study of Fig. 5 also shows that the trend for  $Q_{av}$  is opposite to  $DP_{av}$ , the former is increasing and the latter is decreasing when reducing  $C^*$  from 1 to 0.5  $\text{mol site m}^{-3}$  while keeping the  $k_p$  unchanged. This is because the term of chain transfer rate ( $k_{tr}C^*[H_2]$ ) decreases and monomer concentration in the particle gets higher with lowering of  $C^*$ . This variation will make the monomer concentration predominate and then go up the degree of polymerization

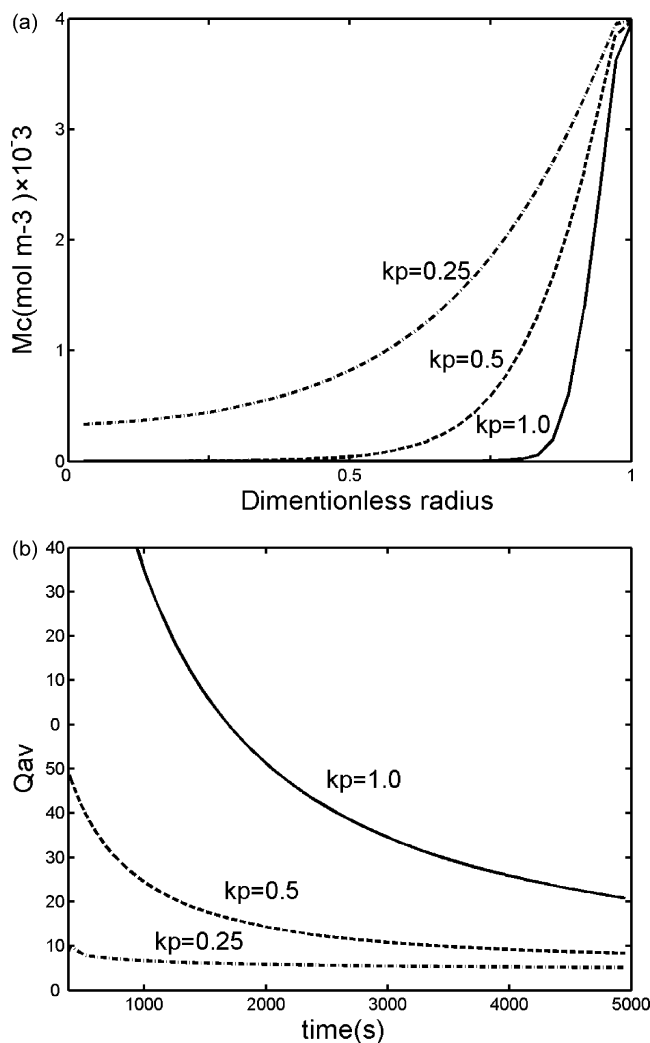


Fig. 4. Effect of change in  $k_p$  on  $M_c$  (a) and  $Q_{av}$  (b).

at the macroparticle level ( $DP_{av}$ ) and reaction rate ( $R_{overall}$ ). It reveals that, therefore,  $DP_{av}$  and  $Q_{av}$  move in the same trend when varying  $k_p$ , while changing in the opposite direction under the influence of  $C^*$ .

### 3.4. Analysis for computational time

The comparison between PMGM and modified PMGM on computational rate is listed in Table 3. It has been shown that the CPU running time of modified model is a little higher than PMGM. Note that over  $N$  algebraic differential equations are added into the modified PMGM by considering the diffusion at microparticle level. It can be seen from the current model that differential Eq. (8) is added in order to figure out the gradient of monomer concentration in the microparticle, namely the monomer concentration ( $M_c$ ) at the surface of subparticle, and other relative equations have to call  $M_c$  which substitutes the original monomer concentration  $M$  simultaneously. Algebraic Eqs. (9), (10),

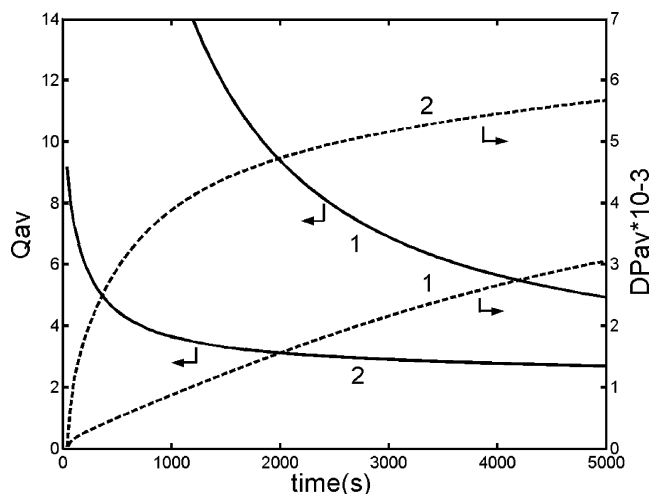


Fig. 5. Effect of change in  $C_x$  while maintaining  $k_p$  unchanged at the level of  $0.5 \text{ m}^3 \text{ mol site}^{-1} \text{ s}^{-1}$  on  $Q_{av}$  (solid line) and  $DP_{av}$  (dash-dot line): (1)  $C_x = 1 \text{ mol site m}^{-3}$  (conference value); (2)  $C_x = 0.5 \text{ mol site m}^{-3}$ .

(14), similarly, are also added for the same purpose mentioned above. In spite of this, the increasing rate is not large enough to affect total computationally efficiency by using this model with the accuracy of results is assured simultaneously and can be convenient for use in more interesting engineering studies like the simulation of different types of polypropylene reactors, optimization, control etc.

## 4. Conclusions

The modified polymeric multigrain model which is based on the experimental observation and some features of both PMGM and MGM indicates the sensitivity of cumulative polydispersity index ( $Q_{av}$ ) to the diffusional constraints and some other parameters is more visibly. It can easily lead the value of  $Q_{av}$  to as high as around 20 when changing some parameters such as  $k_p$ ,  $C^*$  or  $R_c$  even after 1 h polymerization time due to the consideration of monomer diffusion at the microparticle level, not to mention the case of catalyst decay and multiple active site or copolymerization, non-uniformity of catalyst loading and so on [18].

We also amend some unreasonable conclusions of PMGM since the monomer concentration at the centre of the particles drops so quickly to nearly zero and remains

Table 3  
Computational time (Pentium IV 1.7G/256M) for the reference run

Model	Computational time (s)
PMGM (EA with QSSA)	28
PMGM (CSA with QSSA)	4
Modified PMGM (EA with QSSA)	38
Modified PMGM (CSA with QSSA)	6

\*EA indicates the earlier algorithm of PMGM [21].

there for over 2 h of polymerization even though only larger initial catalyst particles can give rise to high PDIs even with higher monomer diffusivities while larger  $R_c$  does not lead to much change in the results with single site catalyst. It has been found from this model, however, that  $DP_{av}$  and PDI are very sensitive to the parameter of  $R_c$  when it has no connection with the total surface area of the microparticle.  $DP_{av}$  and  $Q_{av}$  go in opposite directions, the former increases while the latter decreases when varying  $R_c$  from 0.3 to 0.1  $\mu\text{m}$  at the same value of  $R_0$ . So with single site catalysts, both larger initial catalyst particles and larger subparticles can contribute rise to high PDIs.

This model has also been made computationally very efficient. The corresponding CPU times are pretty much the same level with PMGM and certainly lower significantly than MGM. It is clearly, therefore, convenient for use in more interesting engineering studies like the simulation of different types of polypropylene reactors (continuous stir liquid slurry, liquid loop reactor or fluidized bed etc.), optimization, control etc.

For overall polymerization rate, which is closely related to reactor stability and safety, plays a key role in the propylene polymerization process. Although the value of this parameter obtained by our model is greatly larger than that of PMGM (around 100  $\text{kg kg}^{-1} \text{h}$ ) but it still cannot meet current industrial rate about nearer 100,000  $\text{kg kg}^{-1} \text{h}$  [11]. It is important to indicate, however, that some ideas can be involved which are already developed by Weickert et al. [29] who give a detailed solution on this problem by considering the issue of convection inside growing particles. This work is in progress.

### Acknowledgements

This work is supported by National Natural Science Foundation of China (Grant 20106008), National HI-TECH Industrialization Program of China (Grant Fagai-Gaoji-2004-2080) and Science Fund for Distinguished Young Scholars of Zhejiang University (Grant 111000-581645), and their supports are thereby acknowledged.

### References

- [1] Buls VW, Higgins TL. *J Polym Sci, Polym Chem Ed* 1970;8:1025–35.
- [2] Choi KY, Ray WH. *J Appl Polym Sci* 1985;30:1065–81.
- [3] Dube MA, Soares JBP, Pendilis A, Hamielec AE. *Ing End Chem Res* 1997;36:966–1015.
- [4] Estenez DA, Chiovetta MG. *J Appl Polym Sci* 2001;81:285–311.
- [5] Ferrero MA, Chiovetta MG. *Polym Eng Sci* 1987;27:1436–47.
- [6] Floyd S, Chio KY, Taylor TW, Mann GE, Ray WH. *J Appl Polym Sci* 1986;32:2935–60.
- [7] Floyd S, Herskanen T, Taylor TW, Mann GE, Ray WH. *J Appl Polym Sci* 1987;33:1021–65.
- [8] Galvan R, Tirrell M. *Comput Chem Eng* 1986;10:77–85.
- [9] Hutchinson RA, Chen CM, Ray WH. *J Appl Polym Sci* 1992;44:1389–414.
- [10] Kakugo M, Saadatoshi H, Sakai J, Yokoyama M. *Macromolecules* 1989;22:3172–7.
- [11] Kittilsen P, Svendsen H, McKenna TF. *Chem Eng Sci* 2001;56:3997–4005.
- [12] Laurence RL, Chiovetta MG. *Annu Meet AIChE* 1983;24A.
- [13] McAuley KB, Macdonald DA, McLellan PJ. *AIChE J* 1995;41:868–879.
- [14] McKenna TF, Dupuy J, Spitz R. *J Appl Polym Sci* 1995;57:371–84.
- [15] McKenna TF, Soares JBP. *J Appl Polym Sci* 1997;63:315–22.
- [16] McKenna TF, Soares JBP. *Chem Eng Sci* 2001;56:3931–49.
- [17] Nagel EJ, Krillov VA, Ray WH. *Ind Eng Chem Prod Res Dev* 1980;19:372–9.
- [18] Przybyla J, Zechlin B, Seinmetz B, Tesche B, Fink G. In: Kiminsky W, editor. *Metal organic catalysis for synthesis and polymerization*. Berlin: Springer; 1999. p. 321.
- [19] Ray WH, Villa CM. *Chem Eng Sci* 2000;55:275–90.
- [20] Reginato AS, Zacca JJ, Secchi AR. *AIChE J* 2003;49:2642–54.
- [21] Sarkar P, Gupta SK. *Polymer* 1991;32:2842–52.
- [22] Sarkar P, Gupta SK. *Polymer* 1992;33:1477–85.
- [23] Schmeal WR, Street JR. *AIChE J* 1971;17:1188–97.
- [24] Sheng N, Boyce MC, Parks DM, Rutledge GC, Abes JI, Cohen RE. *Polymer* 2004;45:487–506.
- [25] Singh D, Merrill RR. *Macromolecular* 1971;4:599–604.
- [26] Yermakov YI, Mikhaichenko VG, Besco VS, Grabovski YP, Emirov IV. *Plast Massy* 1970;9:7.
- [27] Yiagopoulos A, Yiannoulakis H, Dimos V, Kiparissides C. *Chem Eng Sci* 2001;56:3979–95.
- [28] Wang AR, Zhu Shiping. *Macromol Theory Simul* 2003;12:196–208.
- [29] Weickert G, Meier GB, Pater TM, Westerterp KR. *Chem Eng Sci* 1999;54:3291–6.
- [30] Xie T, McAuley KB, Hsu CC, Bacon DW. *AIChE J* 1995;41:1251–65.